International Journal of Emerging Science and Engineering (IJESE)
ISSN: 2319–6378, Volume-1, Issue-10, August 2013

Online Condition Monitoring to Diagnose Bearing Faults of Induction Motor

Neelam Mehala

Abstract*—With advances in digital technology over the last years, adequate data processing capabilities is now available on cost effective hardware platforms, to monitor motors for variety of abnormalities on a real time basis. For this reasons, this paper is devoted to investigate the application of advanced signal processing techniques for detection of bearing fault of induction motor. In this study, bearing faults are successfully diagnosed by monitoring the stator current of motor. The experiments were conducted 0.5 hp, 415V induction motor. Virtual instrument was developed with help of programming in software 'LabVIEW'. This instrument was used to obtain the current spectrum of stator current. The different spectrums of healthy motor and faulty motor were than compared to diagnose the bearing faults. The experimental results show that FFT based spectral analysis may be adequate to indicate the presence of bearing faults of induction motors. This may be achieved at a relatively low cost, eliminating need for expensive spectrum analyzers.

Index Terms*— Fault detection, signal processing, motor current signature analysis.

I. INTRODUCTION

The reliability of an induction motor is of paramount importance in industrial, commercial, aerospace and military applications. Bearing play an important role in the reliability and performance of all motor systems. Due to close relationship between motor system development and bearing assembly performance, it is difficult to imagine the progress of modern rotating machinery without consideration of the wide application of bearing. In addition, most faults arising in motors are often linked to bearing faults. The result of many studies show that bearing problems account for over 40% of all machine failure [1].

The bearing consists of mainly of the outer race and inner race way, the balls and cage which assures equidistance between the balls. The different faults occurring in a rolling element bearing can be classified according to the affected element: Outer raceway defect, Inner raceway defect, Ball defect. A fault could be imagined as a small hole, a pit or a missing piece of material on the corresponding elements. Under normal operating conditions of balanced load and a good alignment, fatigue failure begins with small fissures, located between the surface of the raceway and rolling elements, which gradually propagate to the surface generating detectable vibrations and increasing noise levels [2]. Continued stress causes fragments of the material to break loose, producing localized fatigue phenomena known as flaking or spalling [3]. Once started, the affected area expands rapidly contamination the lubricant and causing localized overloading over the entire circumference of the raceway. Some sources such as contamination, corrosion, improper lubrication, improper installation or brinelling reduce the bearing life.

Manuscript received August, 2013.

Neelam Mehala, Department of Electronics Engineering, YMCA University of Science and Technology, Faridabad, INDIA.

Contamination and corrosion are the key factors of bearing failure because of the harsh environments present in most industrial settings. The lubricants are contaminated by dirt and other foreign matter that are commonly often present in the environment of industries. Bearing corrosion is produced by the presence of water, acids, deteriorated lubrication and even perspiration from careless handling during installations. Once the chemical reaction has advanced sufficiently, particles are worn-off resulting in the same abrasive action produced by bearing contamination.

Under and over-lubrication are also some other causes of bearing failure. In either case, the rolling elements are not allowed to rotate on the designed oil film causing increased levels of heating. The excessive heating causes the grease to break down, which reduces its ability to lubricate the bearing elements and accelerates the failure process. In addition, Installation problems are often caused by improperly forcing the bearing onto the shaft or in the housing [3]. This produces physical damage in form of brinelling or false brinelling of the raceways which leads to premature failure.

Regardless of the failure mechanism, defective rolling element bearings generate mechanical vibrations at the rotational speeds of each component. Imagine for example a hole on the outer raceway: as rolling elements move over the defect, they are regularly in contact with the hole which produces an effect on the machine at a given frequency. The next section of this paper demonstrates that these characteristic frequencies which are related to the raceways and the balls or rollers, can be calculated from the bearing dimensions and the rotational speed of the machine.

II. BEARING FAULT ANALYSIS

The bearing consists of mainly of the outer race and inner race way, the balls and cage which assures equidistance between the balls. The different faults that may occur in bearing can be classified according to the affected element [4,5]:

- Outer raceway defect
- Inner raceway defect
- Ball defect

The relationship of bearing vibration to the stator current spectra can be determined by remembering that any air gap eccentricity produces anomalies in the air gap flux density. Since ball bearings support the rotors, any bearing defect will produce a radial motion between the rotor and stator of the machine. The mechanical displacement resulting from damaged bearing causes the machine air gap to vary in a manner that can be described by a combination of rotating eccentricities moving in both directions. Due to rotating eccentricities, the vibrations generate stator currents at frequencies given by [1,3,4,6]:

$$f_{bearing} = \left| f_1 \pm m.f_{i,o} \right| \quad \ldots.(1)$$

where

m=1,2,3,4……..and

$f_{i,o}$ is one of the characteristic frequencies which are based upon the bearing dimensions shown in Figure 1.

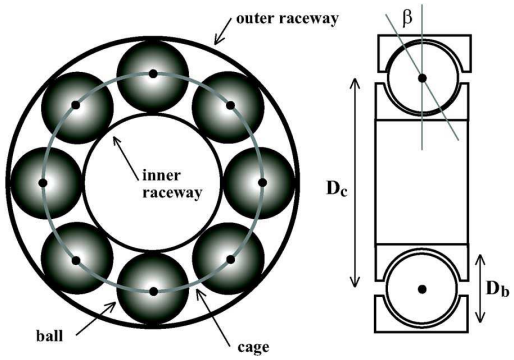

Figure 1: Ball bearing dimensions [1]

$$Outerrace: f_{i,o} = \frac{N_b}{2} f_r \left(1 \pm \frac{D_b}{D_c} \cos\beta\right) \quad \ldots..(2)$$

Where

N_b=number of bearing balls

f_r = mechanical rotor speed in hertz

D_b = Ball diameter

D_c = Bearing pitch diameter

β = Contact angle of the balls on the races

It should be noted from eqn. (2) that specific information concerning the bearing construction is required to calculate the exact characteristic frequencies. However, these characteristics race frequencies can be approximated for most bearings with between six and twelve balls [3,5,6].

$$f_0 = 0.4 N_b f_r \qquad \ldots(3)$$

$$f_i = 0.6 N_b f_r \qquad \ldots.(4)$$

The expected fault frequencies for inner race fault and outer race fault at various load condition are given in Tables I and II.

TABLE I. : EXPECTED FAULT FREQUENCIES FOR INNER RACE FAULT AT VARIOUS LOAD CONDITION

Load Conditions	**Speed (rpm)**	**Slip**	**m=1**		**m=2**		**m=3**	
			LSB (Hz)	*USB (Hz)*	*LSB (Hz)*	*USB (Hz)*	*LSB (Hz)*	*USB (Hz)*
No load	1485	0.01	68	168	187	287	306	406
Full Load	1380	0.08	60	160	170	270	282	382

TABLE II: EXPECTED FAULT FREQUENCIES FOR OUTER RACE FAULT AT VARIOUS LOAD CONDITION

Load Conditions	**Speed (rpm)**	**Slip**	**m=1**		**m=2**		**m=3**	
			LSB (Hz)	*USB (Hz)*	*LSB (Hz)*	*USB (Hz)*	*LSB (Hz)*	*USB (Hz)*
No load	1485	0.01	29	129	108	208	187	287
Full Load	1380	0.08	23	123	97	197	170	270

LSB= Lower Side Band; USB= Upper Side Band

III. BEARING FAULT ANALYSIS USING FFT BASED POWER SPECTRUM

In order to diagnose the bearing fault of induction motor, modern laboratory test bench was used. It consists of three phase induction motor coupled with rope brake dynamometer, transformer, NI data acquisition card PCI-6251, data acquisition board ELVIS and Pentium-IV Personnel Computer with software LabVIEW 8.2. The rated data of the tested three-phase squirrel cage induction machine were: 0.5 hp, 415V, 1.05 A and 1380(FL) r/min. The motor is attached with a rope brake dynamometer. The nominal current is 1.05 A when star connected to 415 V. The bearing of the induction motor are single row, deep groove ball bearing, type 6202-2Z. Each bearing has eight balls. Experiments were conducted on six bearings: two of these are undamaged while four bearing were drilled. Two bearings were drilled through outer race with 'hole diameters' of 2 mm and 4 mm respectively while another two bearing drilled through inner race with 'hole diameter' of 2 mm and 4 mm as illustrated in Figures 2. Bearings of type 6202-2Z were drilled with help of Electric Discharge Machine (EDM) and were installed on motor.

(a) Inner race fault (b) Outer race fault

Figure 2: Inner race fault and outer race fault

A. Data Acquisition Parameters and LabVIEW Programming

To detect the bearing fault, FFT based power spectrums were used. The spectrums were obtained using Virtual instrumentation. The VI was built up by programming in LabVIEW. The VIs was used both for controlling the test measurements and data acquisition, and for the data processing. The stator current is first sampled in the time domain and in the sequence; the power spectrum is calculated and analyzed aiming to detect specific frequency components related to incipient faults. For each bearing fault, there is an associated frequency that can be identified in the spectrum. The faults are detected comparing the amplitude of specific frequencies with that for the same motor considered as healthy. Based on the amplitude in dB it is also possible to determine the degree of faulty condition. The currents that flow in the three phases of induction motor are sensed by current transformer. Current transformer decreased the voltage to 5-10V. This voltage is supplied to ELVIS (National Instrument's data acquisition board). It is then further supplied to National instrument's Data acquisition card. Data acquisition card is connected to PCI slot of Pentium IV personnel computer. The digitalized current signal is applied to the low pass current filter to remove the undesirable high frequency components. Angular velocity of induction motor is measured by a digital tachometer. The 'LabVIEW programme' converts the sampled signal whose frequency is 25000 samples/s to the frequency domain using power spectrum algorithm.

B. Results and discussion

The experiments as given in Table III have been performed to detect bearing faults in three phase induction motor using LabVIEW software. The power spectrum of healthy motor is obtained for all the cases as shown in Figures 3, 8, 11 and 14.

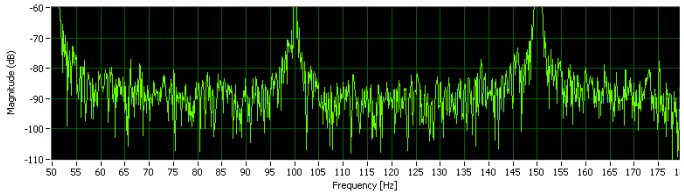

Figure 3: Power spectrum of healthy motor under no load condition

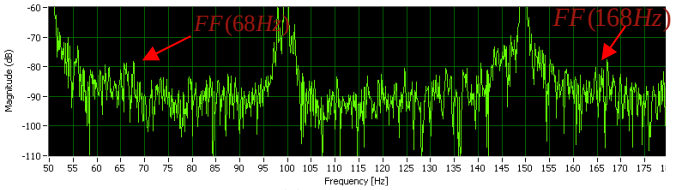

Figure 4: Power spectrum of faulty motor with 2mm hole in inner race of bearing under no load condition (m=1)

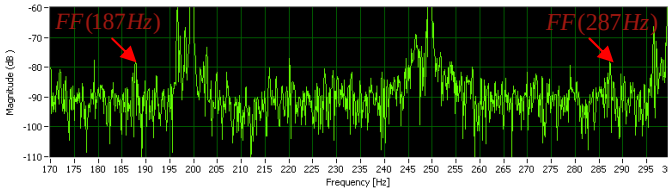

Figure 5: Power spectrum of faulty motor with 2mm hole in inner race of bearing under no load condition (m=2)

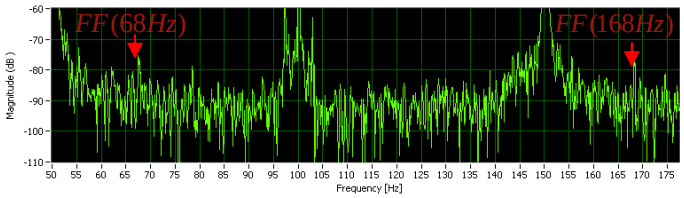

Figure 6: Power spectrum of faulty motor with 4mm hole in inner race of bearing under no load condition (m=1)

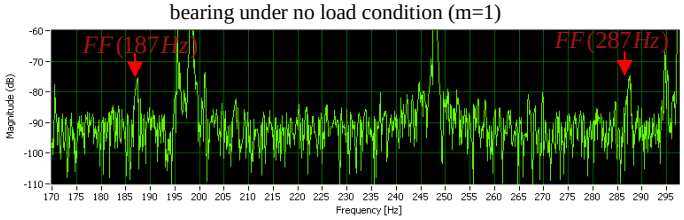

Figure 7: Power spectrum of faulty motor with 4mm hole in inner race of bearing under no load condition (m=2)

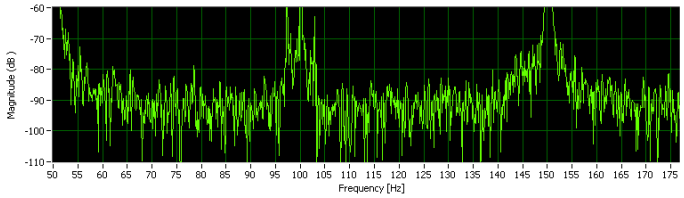

Figure 8: Power spectrum of healthy motor under Full load condition

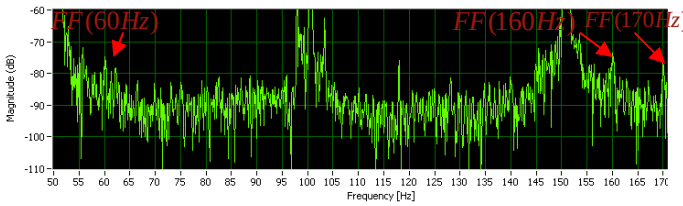

Figure 9: Power spectrum of faulty motor with 2mm hole in inner race of bearing under full load condition

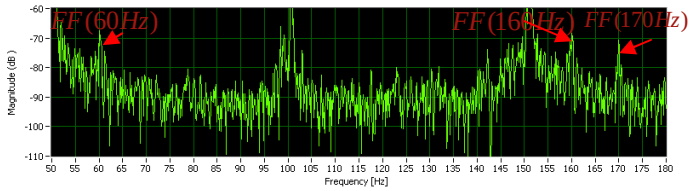

Figure 10: Power spectrum of faulty motor with 4mm hole in inner race of bearing under full load condition

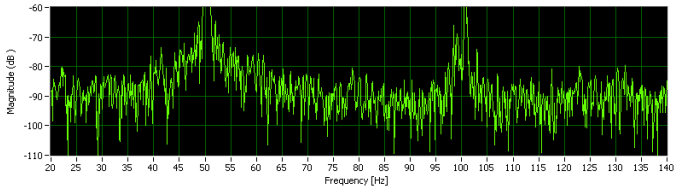

Figure 11: Power spectrum of healthy motor under no load condition

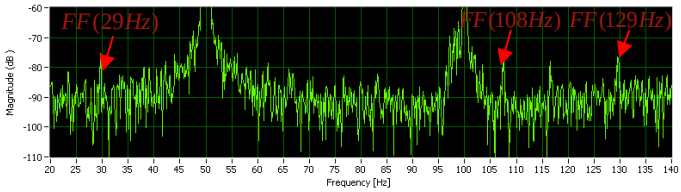

Figure 12: Power spectrum of faulty motor with 2mm hole in outer race of bearing under no load condition

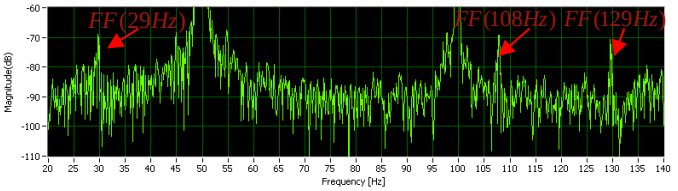

Figure 13: Power spectrum of faulty motor with 4mm hole in outer race of bearing under no load condition

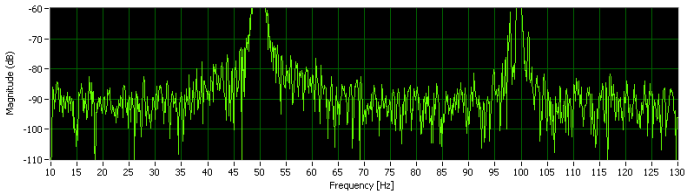

Figure 14: Power spectrum of healthy motor under full load condition

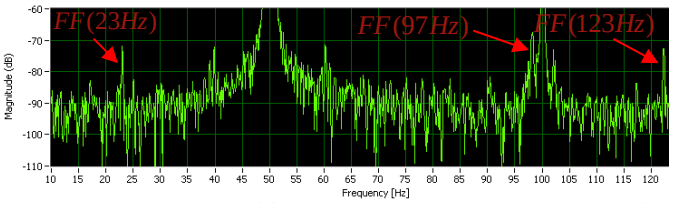

Figure 15: Power spectrum of faulty motor with 2mm hole in outer race of bearing under full load condition

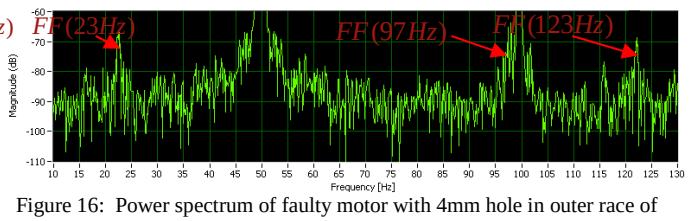

Figure 16: Power spectrum of faulty motor with 4mm hole in outer race of bearing under full load condition

The induction motor is tested with four defective bearings. Defective rolling element bearing generate eccentricity in the air gap with mechanical vibrations. The air gap eccentricity causes variation in the air gap flux density that produces

visible changes in the stator current. These changes are determined in power spectrums of motor due to inner race fault and outer race faults. The outer race faults and inner race faults are diagnosed under no load and full load conditions by conducting some experiments listed in Table III. The results obtained from these experiments are given below:

TABLE III: EXPERIMENTAL CONDITIONS FOR BEARING FAULT DETECTION

Cases	Experiments	Severity of bearing fault	Load conditions
Case 1	1	2mm inner race fault	No Load
	2	2 mm inner race fault	Full load
Case 2	3	4 mm inner race fault	No load
	4	4 mm inner race fault	Full load
Case 3	5	2mm outer race fault	No Load
	6	2 mm outer race fault	Full load
Case 4	7	4 mm outer race fault	No load
	8	4 mm outer race fault	Full load

2 mm inner race fault:

The motor is tested under no load condition with faulty bearing. The fault in bearing was made by drilling a hole of 2mm diameter in its inner race. It is observed from the power spectrums of motor that fault frequencies are not clearly visible at no load condition because their magnitude is less. The power spectrums of faulty motor with 2mm hole in inner race of bearing under no load condition is shown in Figures 4 and 5 When the motor is tested again with same bearing under full load condition, it is observed that magnitude of fault frequencies are increases but these are slightly difficult to identify in the power spectrum. The power spectrum of faulty motor with 2mm hole in inner race of bearing under full load condition is shown in Figures 9. The power spectrums for 2mm inner race fault of motor are shown in Figures 4, 5 and 9 and their analysis for no load and full load is summarized in Table IV.

TABLE IV: POWER SPECTRUM ANALYSIS FOR INNER RACE FAULT OF MOTOR WITH 2MM HOLE

Fig-ure no.	Load Condi-tion	Slip	Fault frequencies						Obser-vations
			FF (Hz)	Mag (dB)	FF (Hz)	Mag (dB)	FF (Hz)	Mag (dB)	
4 and 5	No Load	.01	68	-78	168	-77	187	-78	FF difficult to identify
9	Full Load	.08	60	-76	160	-74	170	-76	FF difficult to identify

4mm inner race fault:

To observe the effect of severity of bearing fault on current components, the 4mm hole was drilled in the inner race and then bearing was installed in the motor. The motor was tested under both no load and full load conditions. The power spectrum of faulty motor with 4mm hole in inner race of bearing under no load condition is shown in Figures 6 and 7. These figures clearly show that the fault frequencies appear at 68 Hz, 168 Hz, 187 Hz and 287 Hz in the spectrum which indicates the inner race fault in the bearing of motor. The magnitudes of these frequencies are between -74 dB to -76 dB.

The motor with same fault was also tested under full load condition. The power spectrum of faulty motor with 4mm hole in inner race of bearing under full load condition is shown in Figure 10. In this case, the fault frequencies appeared at 60 Hz, 160 Hz, and 170 Hz. It is observed that the magnitude of fault frequencies have been increased significantly. It is due to increase of load and severity of fault. The power spectrum analysis for 4mm inner race fault is given in Table V.

2mm outer race fault:

The motor was also tested with outer race fault of bearing. Initially, the 2mm diameter of hole was drilled in the outer race of bearing and then it was installed in the motor. The power spectrum of faulty motor with 2mm hole in outer race of bearing under no load condition is shown in Figure 12. This figure shows that fault frequencies can be clearly identified in power spectrum at 29 Hz, 108 Hz and 129 Hz. Similar results are obtained from the experiment when the motor was tested with same fault under full load conditions. In this case, the fault frequencies are appearing at 23 Hz, 97 Hz and 123 Hz which is indication of outer race fault of bearing. Such frequencies are shown in Figure 15. Table VI gives Power spectrum analysis for induction motor with 2mm outer race fault.

TABLE V: POWER SPECTRUM ANALYSIS FOR INDUCTION MOTOR WITH 4MM INNER RACE FAULT

Fig ure no.	Load Cond-tion	Slip	Fault frequencies						Observations
			FF Hz)	Mag dB)	FF Hz)	Mag (dB)	FF Hz)	Mag dB)	
6 and 7	No Load	0.01	68	-75	168	-74	187	- 76	FF clearly dentified
10	Full Load	0.08	60	-68	160	-68	170	-70	FF clearly dentified

TABLE VI: POWER SPECTRUM ANALYSIS FOR INDUCTION MOTOR WITH 2MM OUTER RACE FAULT

Fig-ure no.	Load Cond-tion	Slip	Fault frequencies						Observation
			FF Hz)	Mag dB)	FF FF)	Mag dB)	FF FF)	Mag dB)	
12	No Load	0.01	29	76	108	74	129	73	FF clearly dentified
15	Full Load	0.08	23	72	97	68	123	73	FF clearly dentified

TABLE VII: POWER SPECTRUM ANALYSIS FOR INDUCTION MOTOR WITH 4MM OUTER RACE FAULT

Fig-u re no.	Load Cond ition	Slip	Fault frequencies						Observation
			FF Hz)	Mag dB)	FF FF)	Mag dB)	FF FF)	Mag dB)	
13	No Load	0.01	29	69	108	69	129	-70	FF clearly dentified
16	Full Load	0.08	23	67	97	65	123	-69	FF clearly dentified

4 mm outer race fault

The motor was again tested with highly defective bearing. In this case, severity of fault was increased to 4mm by drilling the hole into outer race of bearing. The results show that fault frequencies can be clearly identified in power spectrum, when motor is tested under no load condition and full load conditions. The power spectrum of faulty motor with 4mm hole in outer race of bearing under no load

condition is shown in Figure 13. It is observed that the fault frequencies with increased magnitude have been appeared in the power spectrum. The similar results have been obtained, when motor was tested under full load condition. The power spectrum of faulty motor with 4mm hole in outer race of bearing under full load condition is shown in Figure 16. The power spectrum analysis for 4mm outer race fault is given in Table VII.

IV. CONCLUSIONS

This paper investigates the feasibility of detecting the bearing failure using the spectrum of single phase of the stator current of an induction motor. The signal processing technique (Fast Fourier Transform) is used to detect the bearing faults of motor. Experimental results show that the characteristic frequencies could not see in the power spectrum if outer race fault and inner race fault is small in size. As severity of fault increases, the characteristic frequencies become visible. It is clear from the experimental results that FFT based spectral analysis may be adequate to indicate the presence of bearing faults of induction motors. This may be achieved at a relatively low cost, eliminating need for expensive spectrum analyzers.

REFERENCES

[1] R. R. Schoen and T. G. Habetler, and F. Kamran *et al*, "Motor bearing damage detection using stator current monitoring," *IEEE Trans. Ind. Applicat.*, vol. 31, pp. 1280–1286, Nov./Dec. 1995.
[2] Eschmann P, Hasbargen L, Weigand K, "*Ball and roller bearings: Their theory, design, and application"* (London: K G Heyden), 1958.
[3] Riddle J, "Ball bearing maintenance" (Norman, OK: Univ. of Oklohama Press), 1955.
[4] Benbouzid, M. E. H., "A Review of Induction Motors Signature Analysis as a Medium for Faults Detection", *IEEE Transactions on Industrial Electronics*, Vol. 47, October, No. 5,pp. 984-993, 2000.
[5] M. Blodt, P. Granjon, B. Raiso, and G. Rostaing, "Models for bearing damage detection in induction motors using stator current monitoring," *Ind. Electronics, 2004 IEEE International Symposium*, Vol. 1, pp. 383-388, May 2004.
[6] J. R. Stack, T. G. Habetler, and R. G. Harley, "Fault classification and fault signature production for rolling element bearings in electric machines," *IEEE Trans. Ind. Applicat.*, Vol. 40, pp. 735-739, May/June 2004.
[7] Richard G. Lyons, "Understanding digital signal processing", Pearson Education, 2009.
[8] Boashash B., "Time frequency signal analysis" in: Advances in spectrum estimation and array processing, Ed. S. Haykin, *Printice Hall*, 1990.
[9] Leon Cohen, "Time frequency Analysis", Prentice Hall PTR, 1995.
[10] Lokenath Debnath, "Wavelet Transforms and Time Frequency signal analysis", Birkhauser Boston, 2001.

Dr. Neelam Mehala received B.E. degree in Electronics Engineering from N.M. University Jalgaon (M.S.) in 1998. She received M.Tech. Degree in Electronics & Communication Engineering and Ph.D. degree from National Institute of Technology, Kurukshetra in 2002 and 2011 respectively. Currently, she is working as Associate Professor in Electronics and Communication Engineering Department with YMCA University of Science and Technology, Faridabad. Her areas of interest are Signal processing and Fault diagnosis of induction motors.